

Loading and Release of Anti -Cancer Drugs Using Simultaneous pH and Temperature Responsive Nanohybrid

Reza Maleki (✉ rezamaleki96@gmail.com)

USERN <https://orcid.org/0000-0002-5169-5848>

Mohammad Dahri

Shiraz University of Medical Sciences

Hossein Akbarialiabad

shiraz university of medical science

Research article

Keywords: Doxorubicin, Paclitaxel, dimethyl acryl amide-trimethyl chitosan, Molecular dynamic, pH-responsive, hydrogel

Posted Date: December 14th, 2020

DOI: <https://doi.org/10.21203/rs.3.rs-123028/v1>

License:  This work is licensed under a Creative Commons Attribution 4.0 International License.

[Read Full License](#)

Version of Record: A version of this preprint was published at BMC Pharmacology and Toxicology on July 14th, 2021. See the published version at <https://doi.org/10.1186/s40360-021-00508-8>.

Abstract

Background

Today, drug nanocarrier development and improving its biophysical properties is one of the updated and intended of nano-biopharmaceutical science researches. Single-walled carbon nanotubes (SWCNT), as a typical carbon structure based nanocarrier, but have some obstacles in drug delivery mechanisms. In that current study, the penetration, loading, and release of Doxorubicin and Paclitaxel, as two anticancer agents, were investigated using a novel modified and functionalized SWCNT.

Results

This study was carried out using molecular dynamics simulation based on a dual-responsive smart biomaterial. At the *in-silico* study, Interaction energies between drugs and carriers, numbers of hydrogen bonds, diffusion coefficient, and gyration radius were investigated. The kinetic analysis of drug adsorption and release revealed that, fascinatingly, drug loading and drug release are selective at physiological and cancerous acidic pH, respectively. Interaction of Dimethyl acryl amid-trimethyl chitosan, as a biodegradable and biocompatible hydrogel, with SWCNT indicated that degradation reaction in acidic condition destructs the polymer, which leads to a smart release in cancerous tissue at specific pH. Moreover, it resolves hydrophilicity, optimum nanoparticle size, cell membrane penetration, and cell toxicity concerns.

Conclusions

The simulation results indicated a marvelous role of dimethyl acryl amide-trimethyl chitosan in the adsorption and release of anticancer drugs in normal and neoplastic tissue. The interaction of trimethyl chitosan also improves biocompatibility as well as biodegradability of the carrier. Overall, that novel drug carrier can be a virtuous nanoparticle for loading, transporting, and releasing the anticancer drugs.

Background

Cancer, one of the world's major diseases, is a category of genetic diseases implicating odd cell growth which invade or spread to other destination of the body (1, 2). The failure of chemotherapy to have successful selective treatment is a foremost problem in clinical oncology (3, 4). The resistance of neoplastic cells by complex immune escaping mechanisms and specific cancerous micro-environment conditions encourages finding out new strategies (5-8).

Doxorubicin (DOX), as an antibiotic and paclitaxel (PAX) as a herbal medicine, are two significant natural source anticancer drugs in chemotherapy (9, 10). DOX interferes with the production of proteins necessary for the growth of cancer cells, preventing them from reproducing in the body. It appears to act by binding to DNA and inhibiting nucleic acid production by disrupting the molecular structure and by the unique blockage (11-13). Damaging to the normal cells surrounding the cancer tumor and preventing

them from uncontrolled growing, is one of the undesirable side effects of the DOX (14). Targeted drug delivery can minimize the damage of this drug to non-cancerous cells of the body and maximize the efficiency of drug use for cancer treatment (15, 16).

PAX is a microtubule inhibitor that controls the accumulation of microtubules from tubulin dimers and stabilizes the microtubules by preventing depolymerization. This stabilization inhibits the dynamic identification of the microtubule network, which is required for critical interphase and mitotic cellular functions (17-19).

Co-treatment of DOX and PAX is a common and useful regime in cancer therapy so that drug development and side effect reduction of that is exciting and attainable in the clinical oncology. however, the simultaneous release of PAX and DOX has been the subject of many drug studies (20).

Carbon nanostructures are one of the compounds that have recently received much attention in drug delivery (21). Single-walled carbon nanotubes (SWCNT) and 60-carbon fullerenes have a diameter of about 1 nm, half the width of a DNA helix. These particles, due to their small size, can easily cross membranes and biological barriers and reach the infective cell. These structures, with their high surface area, make it easy to modify surface properties using functional groups (22, 23). The surface of these particles is functionalized with various groups and compounds to increase the solubility and biocompatibility, as well as the conductivity of different materials. These particles can be used as carriers for carrying biological molecules such as protein, DNA, and drugs. Medicinal compounds are loaded onto or inside these structures (24). Targeting and transferring two or more compounds simultaneously are other features of interest in drug delivery. Numerous researchers have focused on the potential of carbon nanotubes as carriers for anticancer agents. The unique physical and chemical properties of carbon nanotubes for drug delivery include size, geometric shape, surface charge, surface chemistry, hydrophobicity, in particular, the ability to cross various biological barriers in vivo without producing an immune response (25).

SWCNT can bind with specific cellular receptors and intracellular target molecules for targeted delivery of therapeutic agents (26). Previous studies indicated that the nanotubes enter the cell vertically by the endocytosis process. The nanotubes are also able to pierce the membrane and pass through it because of the needle-like tip, without damaging the cell membrane (27, 28). The drug can be encapsulated into the nanotube and protected while circulating in the body. Upon reaching the target site, the drug is released by the nanotube, and the encapsulating material erodes and disappears. The drug encapsulated inside the nanotube should be proportional to the diameter and size of the nanotube (29, 30). Despite their specific inherent properties, concerns have transpired apropos the toxicity of CNTs, as several studies have manifested that pristine nanotubes could instigate biological destruction.

In that work, CNT Bioconjugation with a novel biodegradable and biocompatible polymer dispel its biological concerns and make a safer and more reliable nanocarrier. On the other hand, An extensive range of investigation has also indicated that development of nanotube by functionalized with carboxylic group make it better in pharmacodynamics and pharmacokinetic properties of drug delivery ,overall in

that work the pH-responsive CNT modified with non-bonded interaction of dimethyl Acryl amide-trimethyl chitosan (DMMA-TMC), as a biopolymer, produce a biocompatible CNTs which capable of local, smart and target delivery systems to cancerous tissue. DMMA-TMC, as a modified polysaccharide from chitosan, plays a decisive role in adsorption enhancing in novel macromolecule delivery systems (31). Moreover, its non-bonded interaction with Carbon nanotube and positively charged induce the specific properties in drug adsorption and drug release. Taking advantage of the adsorption enhancing the effect of DMMA-TMC, TMC@CNT were evaluated as potential vehicles to improve the loading of PAX and DOX in the physiological pH (32).

Molecular dynamics is a powerful tool that can provide qualitative and quantitative information on the physicochemical interactions and mechanisms of pharmaceutical systems and is more attractive from machine learning methods (33-35). In the study of molecular dynamics, a system consisting of nanoparticles inside a box, called a computational box, is first considered. Knowing the location and velocity of the particles at each step can calculate all the static and dynamic properties of the system. From the theorist's point of view, the importance of molecular dynamics studies is that they provide accurate quasi-experimental results for a well-defined model. Molecular dynamics provides an intermediary between laboratory experiments and theory and is considered a pragmatic trial (36, 37).

Because of the difficulties and high cost of empirical experiments, there are many studies today on molecular dynamics to simulate drug delivery systems in cancer (38). Few studies have been done on DOX and PAX with novel nanocarriers using molecular dynamics. Molecular dynamics has been investigated for the release of DOX, including graphene and graphene oxide carriers (39, 40). In that work, the effects of pH, molecular bonds, carrier size, and functional groups have been investigated. Previous studies have not investigated the mechanism of DOX-PAX adsorption, penetration, and release from this modified type of carbon nanotubes using molecular dynamics. Current work investigates carbon nanotubes as an attractive nanocarrier for drug release, and drug loading, cell membrane penetration, and release of DOX and PAX from SWCNT and introduces carbon nanotubes as a suitable carrier for DOX and PAX drug delivery. Given the unique properties of carbon nanotubes, this could be a good introduction to the greater use of carbon nanotubes in loading and release of anticancer drugs.

Results And Discussion

Different mechanisms of DOX and PAX were studied in two physiological (pH=7.4) and cancerous (pH=5.5) conditions to predict cellular penetration, adsorption, and release.

1- Drug adsorption in neutral condition (pH=7.4)

In the **fig.1.**, the interaction of the DOX molecule with the single-walled nanotube is investigated. As shown in the figure at neutral pH, electrostatic energy plays a significant part in the total interaction energy. While in the acidic state, the electrostatic energy is zeroed, and the van der Waals energy has a considerable share of the total interaction energy. This is due to the surface charge of the carboxyl

functional groups at the nanotube surface. Because the nanotube is functionalized with carboxyl functional groups. The carboxyl group has a negative charge at neutral pH and no charge at acidic pH.

On the other hand, DOX has a positive charge at both neutral pH and acidic pH. As a result, in the neutral state, drug functional groups and nanotube have anonymous charges, and there are robust electrostatic interactions. The higher the electrostatic energy at neutral pH, the higher the adsorption of the drug onto the nanocarrier surface at this pH. The important thing is that the drug at a neutral pH, which is the pH of the blood, can transfer well to the surface of the nanotube, and the nanotube, having a strong attraction to the DOX drug, is an excellent carrier for this drug.

The following figure(fig.1.) shows the interaction between DOX and chitosan. As it is evident from the picture, the Van der Waals force is close to zero, but there is a considerable negative electrostatic interaction between the drug and the chitosan. This interaction is due to the positive charge of DOX and the negative charge of chitosan at this pH. The negative electrostatic energy indicates a strong attraction between the drug and the chitosan. Chitosan is a critical aid in the adsorption of the drug.

In the following (Fig.2.), the energy interaction of PAX with single-walled nanotubes is investigated. As shown in the figure at neutral pH, van der Waals energy shows a more significant number, and electrostatic energy is close to zero. The nanotubes are functionalized with carboxyl functional groups. The carboxyl group has a negative charge at neutral pH and no charge at acidic pH. On the other hand, PAX has zero charges at neutral pH. As a result, in the neutral state, the electrostatic energy between PAX and the nanotube is close to zero. Van der Waals Energy plays a significant part in the uptake of PAX on carbon nanotubes.

On the other hand, Fig.2. Showed the energy interaction of PAX with chitosan. As shown in the figure at neutral pH, van der Waals energy shows a more significant number, and electrostatic energy is close to zero. PAX has zero charges at neutral pH. As a result, in the neutral state, the electrostatic energy between PAX and chitosan is close to zero. Van der Waals Energy has a significant contribution to the uptake of PAX on chitosan. Hydrogen bonds, which is a significant factor in drug delivery. A comparison between PAX and DOX shows that the DOX-chitosan hydrogen bonds are stronger than the PAX-chitosan hydrogen bonds. Therefore, the addition of chitosan also contributes to better adsorption of DOX because the strength of the hydrogen bonds between DOX and chitosan is relatively high.

Table.1: Number of Averages H bonds-average

| | DOX-CNT | DOX-TMC | PAX-CNT | PAX-TMC |
|----------------|---------|---------|---------|---------|
| pH= 7.4 | .007 | 2.707 | 0 | 0.342 |
| pH=5.5 | 0 | 0.071 | 0.189 | 0.112 |

2- Drug release in acidic condition (pH=5.5)

In the following figure, **Fig.3.** The interaction of the DOX molecule with single-walled nanotube nanocarriers is investigated. As shown in the picture at acidic pH, the electrostatic energy is shallow and close to zero. At acidic pH, electrostatic energy is zero, and van der Waals energy has a significant contribution to the total interaction energy. This is due to the surface charge of the carboxyl functional groups on the nanotube surface. The nanotube is functionalized with carboxyl

functional groups. The carboxyl group has a negative charge at neutral pH and no charge at acidic pH.

On the other hand, DOX has a positive charge at neutral pH and acidic pH. As a result, in the neutral state, drug functional groups and nanotube have anonymous and find strong electrostatic interactions. However, at acidic pH, nanotube and carboxyl group charges become zero. Furthermore, the electrostatic interaction energy between the nanotube and DOX is also zero.

The higher energy of the double-walled nanotubes than the single-walled nanoparticles and fullerene indicates that the double-walled nanotubes are a stronger absorbent for DOX at this pH. Furthermore, after that, single-walled nanotubes can absorb DOX molecules better than fullerene.

The following figure (Fig.3.) shows the interactions between DOX and chitosan polymer. The interesting point in the diagram below is that the interaction between the drug and the chitosan in an acidic state has positive electrostatic energy. This means that there is a repulsion between chitosan and the drug, and this is very effective in releasing the drug. Repulsion between chitosan and drug causes the better release of drug from chitosan and nanotube surface. In fact, besides biocompatibility and hydrophilicity, chitosan plays a critical role in the mechanism of drug release in cancer tissue.

The figure (**Fig.4.**) shows van der Waals and electrostatic interaction between PAX and nanotube. As is clear from the picture, the electrostatic energy is close to zero, and the total energy is approximately equivalent to the van der Waals energy. The loss of electrostatic energy is due to the zero charge of the carboxyl group at acidic pH. Moreover, the surface charge of the PAX is close to zero. Therefore, the electrostatic interaction between PAX and the nanotube is zero, and the van der Waals interaction is fragile. The weak interaction energies lead to a better release of the drug from the nanotubes and are considered a decisive factor for the carrier, which can be very useful in drug release.

Also, The last figure Fig.4. shows the interaction energy between PAX and chitosan in an acidic state. As can be seen from the figure, the electrostatic and van der Waals interaction between the drug and the chitosan is zero, which helps the drug release. The zero electrostatic energy is due to the zero-surface charge of PAX.

Hydrogen bonding between two atoms is defined as a receiver-acceptor pair with an angle between them less than 30 degrees. The graph of changes in the number of hydrogen bonds over time between the polymer-polymer and polymer-drug and CNT-drug for all three simulations are shown in the diagrams below. Hydrogen bonds indicate the amount of hydrophilicity property of carriers. Besides, hydrogen bonding is part of the interatomic forces that can contribute to carrier strength and stability. The

following diagrams at Fig.1. And Fig.3. Show that DOX is not bound to CNT but has many hydrogen bonds with TM-chitosan polymer. This chart illustrates the crucial role of chitosan in this drug delivery system. Because chitosan forms carriers more hydrophilic through hydrogen bonding formation. CNTs and DOX, as well as PAX, are hydrophobic compounds, and this is a significant drawback for pharmaceutical carriers. Because hydrophobic compounds aggregate in water and form larger particles that disrupt drug delivery and block the bloodstream. However, Chitosan has solved this problem by hydrophilizing the complex. The graphs in Fig.2. and Fig.4. also show that PAX did not form eligible hydrogen bonds with CNT, while the same drug with chitosan has many.

3- Cell penetration

Gyration radius is a factor that enables the aggregation of molecules such as polymers, resizing of biological macromolecules such as proteins over time. The diagram of the gyration radius is shown below. As shown in the figure below (Fig.5.), the gyration radius indicates the accumulation of polymer molecules in one region. The higher the gyration radius, the greater the dispersion between the molecules. The gyration radius of DOX and PAX is about 3 nm, indicating the complex radius of drug accumulation on the fullerene surface. Due to the fullerenes and box simulations, a useful aggregation of drugs is formed around the SWCNT. This indicates that the polymer molecules are clustered together in this simulation. PAX also has a lower radius than DOX, indicating a better accumulation of PAX than DOX. Complexation due to the accumulation of PAX molecules is more stable and concentrated.

4- radial distribution function

The following diagrams show the radial distribution function of DOX and PAX in the simulation box. For both layouts, there is a steep slope of the graph and peak. Where the peak diagram is seen, and the RDF is high, the accumulation of drug molecules has occurred. This indicates that the drug molecules are aggregated at one point and are concentrated at the same spot and are not distributed in the simulation box. This result corroborates previous results suggesting acceptable drug adsorption on fullerenes and polymers.

5- drug diffusion coefficient

The slope of the mean square displacement curve represents the diffusion coefficient. This chart shows the diffusion coefficient of DOX in the simulation box. The steric hindrance is less an acidic state. Because the adsorption of the drug on the fullerene surface is less, so their accumulation is lower than that of the neutral state, and as a result, the number of collisions and steric hindrance is less.

Eventually, the reduction of the steric hindrance will increase the diffusion coefficient. So, in the acidic state, the drug diffusion rate is higher.

Conclusion

DOX and PAX are anticancer drugs that have been the subject of plentiful research in vitro studies on drug delivery systems to cancer cells. Molecular drug delivery studies of DOX-based on carbon nanotubes have been the subject of this study, which has shown that carbon nanotubes can be a suitable carrier for these drugs through the mechanism of pH change. In this computational work, the interactions between DOX and PAX with single-walled nanotubes at different acidic and neutral pHs were investigated.

By applying molecular dynamic simulation, The results indicate the appropriate uptake of the drug occurs at neutral pH (which is the normal pH of human blood), and its optimal release occurs at acidic pH (which is the normal pH of the cancerous tissue environment). The effect of dimethyl acrylamide trimethyl chitosan in this work was investigated, and it was found that chitosan plays a vital role in the release of DOX and the uptake of PAX. Chitosan also helps to make this carrier more biocompatible.

Fantastically, The results reveal that the combination of nanotubes and chitosan is useful for simultaneous adsorption and release of DOX and PAX.

As a suggestion for future work, this system can be tested in the laboratory environment as well as in the tissue of living organisms.

Methods

The basis of the molecular dynamics work is the numerical integration of Newton's equations of motion for every single particle in the system. By applying Newton's equations of motion, a set of atomic positions is obtained successively. By using molecular dynamics, the state and properties of the system at any later time can be predicted from its current state. The molecular dynamics consists of the following three steps:

1. Obtaining the initial particle configuration, which is the initial coordinates of the atoms and the initial velocities and physical properties such as the mass, size, and type of atom.
2. Computing the list of neighbors. This list is compiled for each atom in the system and includes all atoms in the range of the particle's power. The list of neighbors changes every time.
3. Calculating the force applied to each atom based on the configuration and initial conditions and calculation of the acceleration of each particle and obtain the new velocity and location of each particle using one of the integration methods. The continuous nature of more realistic potentials requires that Newton's equations of motion be integrated by breaking the calculation into a set of short time steps (between 1 and 10 femtoseconds). At each level, the forces acting on the atoms are calculated and combined with current positions and velocities to obtain new positions and velocities within a short time. The force which acts on each atom is assumed to be constant over this time interval. Therefore, atoms are moved to new positions, a set of forces is calculated, and the process is repeated. As such, molecular dynamics simulation calculates a path that describes how dynamical variables change over time

1- Molecular dynamics

In order to perform molecular dynamics simulations, GROMACS 5.1.2 software was used for input structures with the oplsa force field. To obtain the parameters of the molecule that were converted to GROMACS format using ACPYPE script. All the molecules were placed inside the box, and the tip3p water model was used as the solvent. Energy reduction was performed on all 50,000-step simulation systems by the steepest descent method to eliminate van der Waals interactions and to form hydrogen bonds between water molecules and other molecules. In the next step, the system temperature gradually increased from 0 to 310 K for 100 picoseconds in constant volume, using the Nose-Hoover algorithm as well as the temperature system coupling rate of 0.5ps and then at the constant pressure was equilibrated for 200 picoseconds. The Parrinello-Rahman algorithm was used to balance the system pressure. Molecular dynamics simulation was performed at 37 ° C for 50 ns. The cut-off distance was set at 1.2. Particle mesh Ewald (pme) was used to calculate the electrostatic force. The LINear Constraint Solver algorithm was used to maintain the length of all links. In order to increase the computational speed, the SHAKE algorithm was used to limit the bonds involved in the hydrogen atom

To calculate the permeability coefficient of the drug in the square vector, we calculate the mean displacement of the atoms with 'r', and 't' represents time. The following formula shows the mean square of the displacement:

$$\text{MSD} = \langle [\mathbf{r}(t) - \mathbf{r}(0)]^2 \rangle = \frac{1}{t} \sum_{t=t_0}^t [\mathbf{r}(t) - \mathbf{r}(0)]^2 \quad (1)$$

After calculating the MSD, the diffusion coefficient for the three-dimensional system can be derived from Einstein's relation.

$$D = \frac{1}{6} \lim_{t \rightarrow \infty} \frac{\text{MSD}}{t} \quad (2)$$

2- Carbon nanotubes simulation

TubeGen Online web server was used to make a single wall and double wall nanotube molecules. Carbon dioxide molecules were added to the nanotube surface in both protonated and deprotonated states. The carbon atom charge in these nanostructures was assumed based on the use of naphthalene structure in the zero oplsa force field. The types of bonds between carbon atoms were defined based on amino acids phenylalanine (Phe), tyrosine, and tryptophan (Trp). The angle type is also determined using the angles of the aromatic amino acid phenylalanine ring. The charge and parameters of the functional groups on this nanostructure were defined based on the similar structure existing in the Optimized Potentials for Liquid Simulation-all atom (OPLS-aa) force field. Lenard-Jones models and Columbian potentials were used to calculate non-bonding interactions such as van der Waals and electrostatic, respectively.

Abbreviations

| | |
|----------|---|
| Phe | phenylalanine |
| Trp | tryptophan |
| OPLS-aa | Optimized Potentials for Liquid Simulation-all atom |
| Pme | Particle mesh Ewald (|
| MSD | mean square of the displacement: |
| DMMA-TMC | dimethyl Acryl amide-trimethyl chitosan |
| DOX | doxorubicin |
| PAX | paclitaxel |
| SWCNT | Single-walled carbon nanotubes |
| RDF | radial distribution function |

Declarations

Ethics approval and consent to participate

Not applicable

Consent for publication

Not applicable

Availability of data and materials

The datasets used and/or analyzed during the current study are available from the corresponding author on reasonable request.

Competing interests

The authors declare that they have no competing interests

Funding

Not applicable

Authors' contributions

RM and MD simulated and interpreted the data regarding the softwares. RM and MD performed the analysis and data virtualizations of the drug delivery system, and HA was a major contributor in writing the manuscript. All authors read and approved the final manuscript.

Acknowledgements

All authors thanks Ehsan Alimohammadi to editing the language of article.

References

1. Pantel K, Speicher M. The biology of circulating tumor cells. *Oncogene*. 2016;35(10):1216.
2. Sawyers C. Targeted cancer therapy. *Nature*. 2004;432(7015):294.
3. Demetri GD, Von Mehren M, Jones RL, Hensley ML, Schuetze SM, Staddon A, et al. Efficacy and safety of trabectedin or dacarbazine for metastatic liposarcoma or leiomyosarcoma after failure of conventional chemotherapy: results of a phase III randomized multicenter clinical trial. *Journal of Clinical Oncology*. 2016;34(8):786.
4. Tang X, Xu X, Han Z, Bai G, Wang H, Liu Y, et al. Elaboration of a multimodal MRI-based radiomics signature for the preoperative prediction of the histological subtype in patients with non-small-cell lung cancer. *Biomedical engineering online*. 2020;19(1):5.
5. Cheng Y-J, Qin S-Y, Ma Y-H, Chen X-S, Zhang A-Q, Zhang X-Z. Super-pH-Sensitive Mesoporous Silica Nanoparticle-Based Drug Delivery System for Effective Combination Cancer Therapy. *ACS Biomaterials Science & Engineering*. 2019;5(4):1878-86.
6. Gao C, Tang F, Gong G, Zhang J, Hoi MP, Lee SM, et al. pH-responsive prodrug nanoparticles based on a sodium alginate derivative for selective co-release of doxorubicin and curcumin into tumor cells. *Nanoscale*. 2017;9(34):12533-42.
7. Beatty GL, Gladney WL. Immune escape mechanisms as a guide for cancer immunotherapy. *Clinical cancer research*. 2015;21(4):687-92.
8. Seshadri DR, Ramamurthi A. Nanotherapeutics to modulate the compromised micro-environment for lung cancers and chronic obstructive pulmonary disease. *Frontiers in Pharmacology*. 2018;9.
9. Molinski TF, Dalisay DS, Lievens SL, Saludes JP. Drug development from marine natural products. *Nature reviews Drug discovery*. 2009;8(1):69.
10. Sikov WM, Berry DA, Perou CM, Singh B, Cirrincione CT, Tolaney SM, et al. Impact of the addition of carboplatin and/or bevacizumab to neoadjuvant once-per-week paclitaxel followed by dose-dense doxorubicin and cyclophosphamide on pathologic complete response rates in stage II to III triple-negative breast cancer: CALGB 40603 (Alliance). *Journal of clinical oncology*. 2015;33(1):13.
11. Taymaz-Nikerel H, Karabekmez ME, Eraslan S, Kirdar B. Doxorubicin induces an extensive transcriptional and metabolic rewiring in yeast cells. *Scientific reports*. 2018;8(1):13672.
12. Renu K, Abilash V, PB TP, Arunachalam S. Molecular mechanism of doxorubicin-induced cardiomyopathy–An update. *European journal of pharmacology*. 2018;818:241-53.
13. Wang Y, Xu Z. Interaction mechanism of doxorubicin and SWCNT: protonation and diameter effects on drug loading and releasing. *RSC advances*. 2016;6(1):314-22.

14. Van Norren K, Van Helvoort A, Argiles J, Van Tuijl S, Arts K, Gorselink M, et al. Direct effects of doxorubicin on skeletal muscle contribute to fatigue. *British journal of cancer*. 2009;100(2):311.
15. Tang J, Zhang R, Guo M, Shao L, Liu Y, Zhao Y, et al. Nucleosome-inspired nanocarrier obtains encapsulation efficiency enhancement and side effects reduction in chemotherapy by using fullerene assembled with doxorubicin. *Biomaterials*. 2018;167:205-15.
16. Khoshoei A, Ghasemy E, Poustchi F, Shahbazi M-A, Maleki R. Engineering the pH-Sensitivity of the Graphene and Carbon Nanotube Based Nanomedicines in Smart Cancer Therapy by Grafting Trimethyl Chitosan. *Pharmaceutical Research*. 2020;37(8):160.
17. Gomez IJ, Arnaiz B, Cacioppo M, Arcudi F, Prato M. Nitrogen-doped carbon nanodots for bioimaging and delivery of paclitaxel. *Journal of Materials Chemistry B*. 2018;6(35):5540-8.
18. Maleki R, Khoshoei A, Ghasemy E, Rashidi A. Molecular insight into the smart functionalized TMC-Fullerene nanocarrier in the pH-responsive adsorption and release of anti-cancer drugs. *Journal of Molecular Graphics and Modelling*. 2020;100:107660.
19. Qu N, Sun Y, Li Y, Hao F, Qiu P, Teng L, et al. Docetaxel-loaded human serum albumin (HSA) nanoparticles: synthesis, characterization, and evaluation. *Biomedical engineering online*. 2019;18(1):11.
20. Yeung CLA, Co N-N, Tsuruga T, Yeung T-L, Kwan S-Y, Leung CS, et al. Exosomal transfer of stroma-derived miR21 confers paclitaxel resistance in ovarian cancer cells through targeting APAF1. *Nature communications*. 2016;7:11150.
21. Pardo J, Peng Z, Leblanc RM. Cancer targeting and drug delivery using carbon-based quantum dots and nanotubes. *Molecules*. 2018;23(2):378.
22. Bafkary R, Khoee S. Carbon nanotube-based stimuli-responsive nanocarriers for drug delivery. *RSC Advances*. 2016;6(86):82553-65.
23. Mehra NK, Jain K, Jain NK. Pharmaceutical and biomedical applications of surface engineered carbon nanotubes. *Drug Discovery Today*. 2015;20(6):750-9.
24. He X, Gao W, Xie L, Li B, Zhang Q, Lei S, et al. Wafer-scale monodomain films of spontaneously aligned single-walled carbon nanotubes. *Nature nanotechnology*. 2016;11(7):633.
25. Dineshkumar B, Krishnakumar K, Bhatt A, Paul D, Cherian J, John A, et al. Single-walled and multi-walled carbon nanotubes based drug delivery system: Cancer therapy: A review. *Indian journal of cancer*. 2015;52(3):262.
26. Costa PM, Bourgoignon M, Wang JT, Al-Jamal KT. Functionalised carbon nanotubes: from intracellular uptake and cell-related toxicity to systemic brain delivery. *Journal of Controlled Release*. 2016;241:200-19.
27. Yaron PN, Holt BD, Short PA, Lösche M, Islam MF, Dahl KN. Single wall carbon nanotubes enter cells by endocytosis and not membrane penetration. *Journal of nanobiotechnology*. 2011;9(1):45.
28. Pérez-Luna V, Moreno-Aguilar C, Arauz-Lara JL, Aranda-Espinoza S, Quintana M. Interactions of Functionalized Multi-Wall Carbon Nanotubes with Giant Phospholipid Vesicles as Model Cellular Membrane System. *Scientific reports*. 2018;8(1):17998.

29. del Carmen Giménez-López M, Moro F, La Torre A, Gómez-García CJ, Brown PD, Van Slageren J, et al. Encapsulation of single-molecule magnets in carbon nanotubes. *Nature communications*. 2011;2:407.
30. Ashokkumar AE, Enyashin AN, Deepak FL. Single walled Bil 3 nanotubes encapsulated within carbon nanotubes. *Scientific reports*. 2018;8(1):10133.
31. Ways M, Mohammed T, Lau WM, Khutoryanskiy VV. Chitosan and its derivatives for application in mucoadhesive drug delivery systems. *Polymers*. 2018;10(3):267.
32. Li Q, Zhou G, Yu X, Wang T, Xi Y, Tang Z. Porous deproteinized bovine bone scaffold with three-dimensional localized drug delivery system using chitosan microspheres. *Biomedical engineering online*. 2015;14(1):1-15.
33. Comer J, Chen R, Poblete H, Vergara-Jaque A, Riviere JE. Predicting adsorption affinities of small molecules on carbon nanotubes using molecular dynamics simulation. *ACS nano*. 2015;9(12):11761-74.
34. Rezvantalab S, Keshavarz Moraveji M, Khedri M, Maleki R. An insight into the role of riboflavin ligand in the self-assembly of poly(lactic-co-glycolic acid)-based nanoparticles – a molecular simulation and experimental approach. *Soft Matter*. 2020;16(22):5250-60.
35. Sahooli M, Sabbaghi S, Maleki R, Nematollahi MM. Thermal conductivity of Water-based nanofluids: Prediction and comparison of models using machine learning. *International Journal of Nano Dimension*. 2014;5(1):47-55.
36. Mahdavi M, Rahmani F, Nouranian S. Molecular simulation of pH-dependent diffusion, loading, and release of doxorubicin in graphene and graphene oxide drug delivery systems. *Journal of Materials Chemistry B*. 2016;4(46):7441-51.
37. Alimohammadi E, Khedri M, Miri Jahromi A, Maleki R, Rezaian M. Graphene-Based Nanoparticles as Potential Treatment Options for Parkinson's Disease: A Molecular Dynamics Study. *Int J Nanomedicine*. 2020;15:6887-903.
38. Venable RM, Krämer A, Pastor RW. Molecular dynamics simulations of membrane permeability. *Chemical reviews*. 2019;119(9):5954-97.
39. Nedyalkova M, Romanova J, Stoycheva J, Madurga S. Simulation Paths of Anticancer Drugs on a Graphene Oxide Surface. *Graphene Functionalization Strategies*: Springer; 2019. p. 215-28.
40. Hashemzadeh H, Raissi H. Understanding Loading, Diffusion and Releasing of Doxorubicin and Paclitaxel Dual Delivery in Graphene and Graphene Oxide Carriers as Highly Efficient Drug Delivery Systems. *Applied Surface Science*. 2019:144220.

Figures

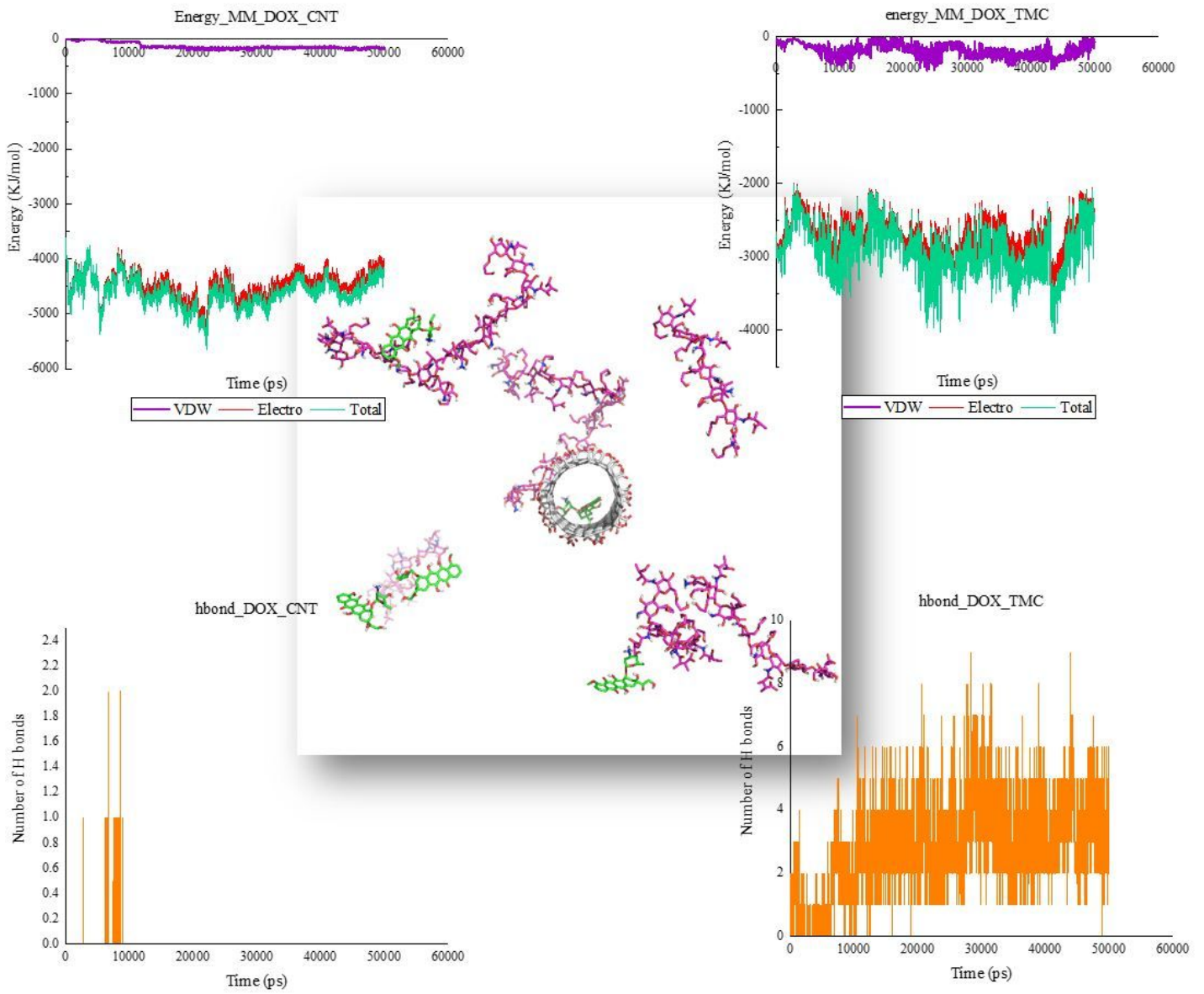


Figure 1

Interaction between CNT and DOX; pH=7.4

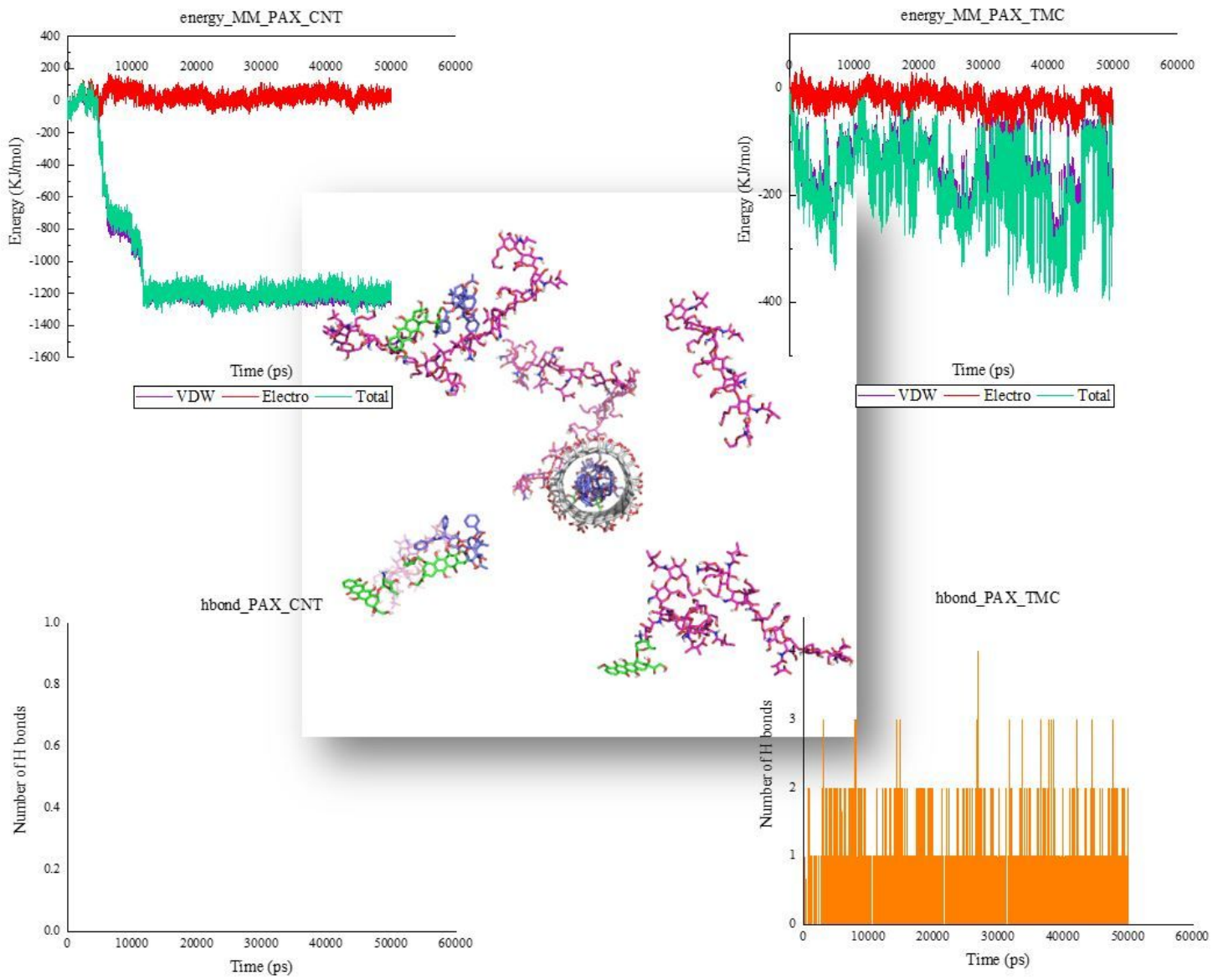


Figure 2

Interaction between CNT and PAX; pH=7.4

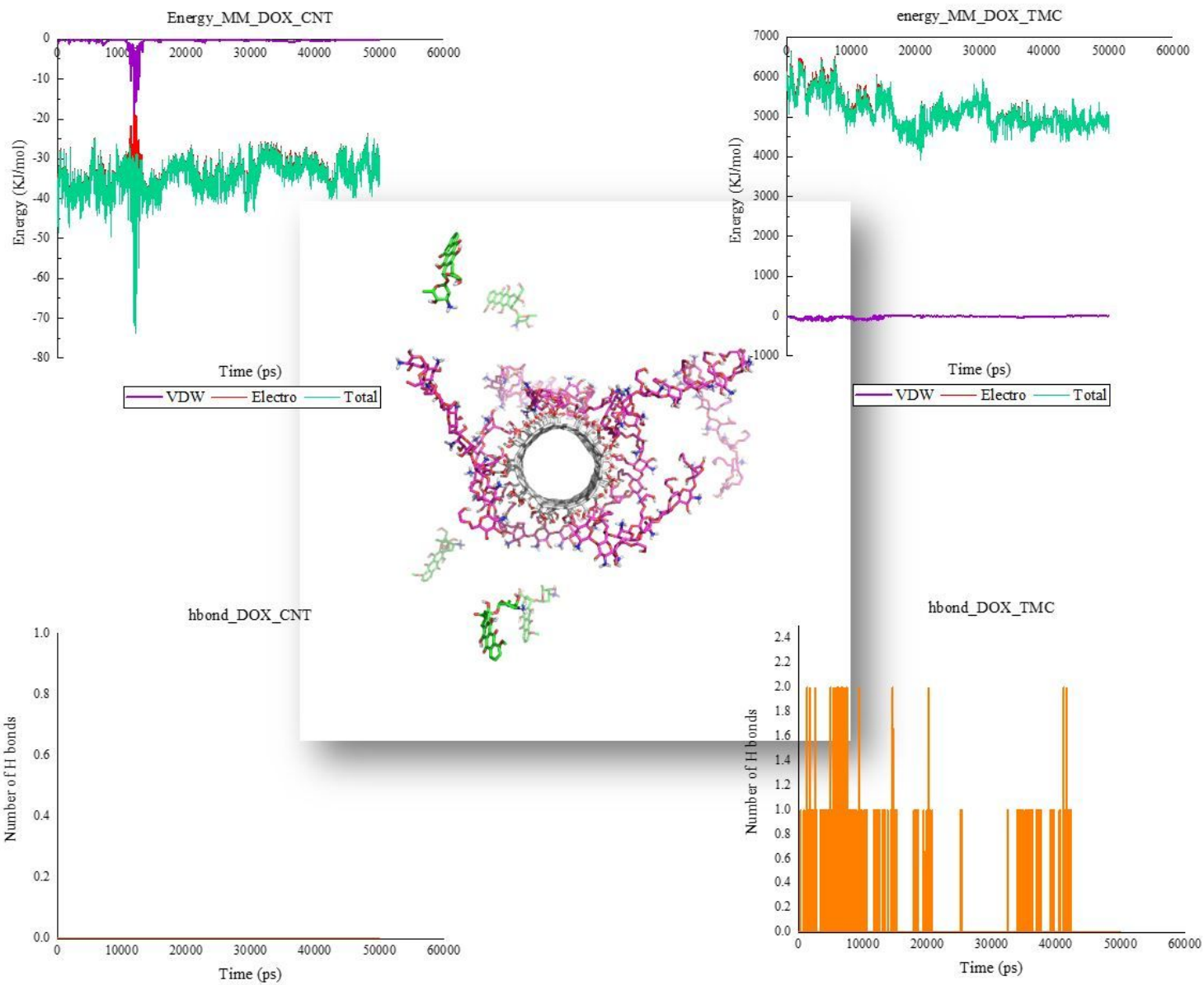


Figure 3

Interaction between CNT and DOX; pH=5.5

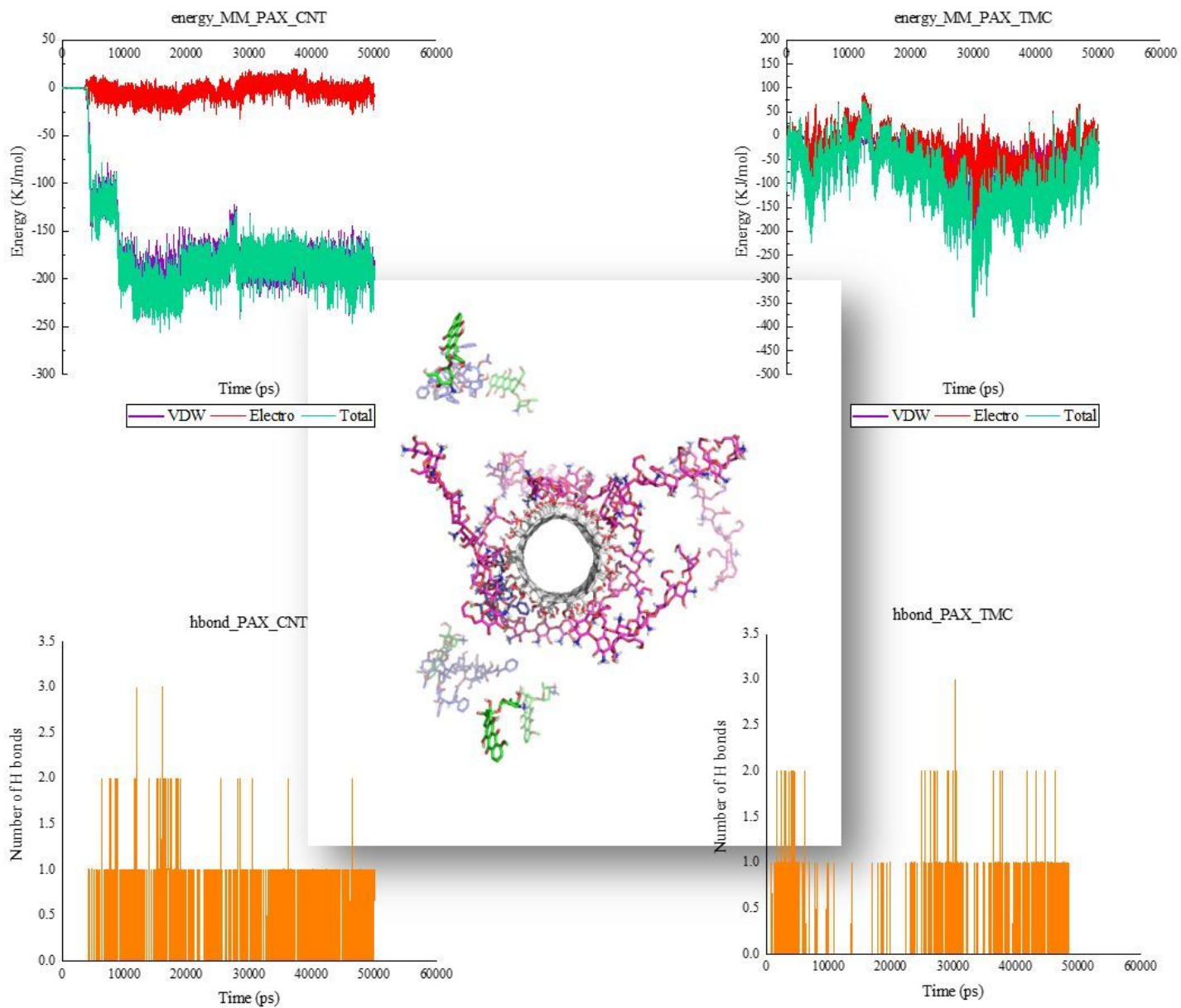


Figure 4

Interaction between CNT and PAX; pH=5.5

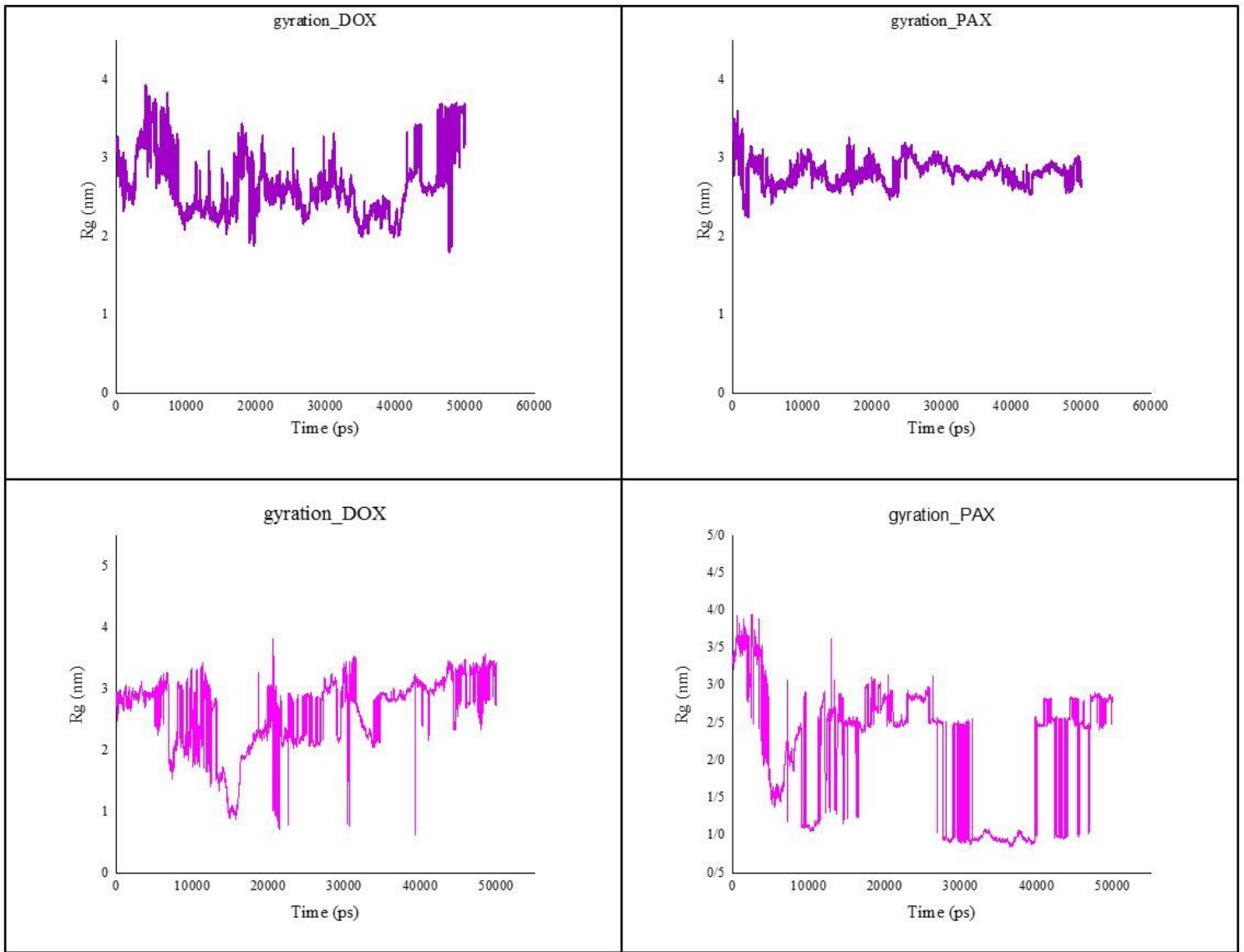


Figure 5

Gyration radius of Drugs and carrier; a: DOX pH=7.4 b: PAX pH7.4 c: DOX pH=5.5 d: PAX pH=5.5

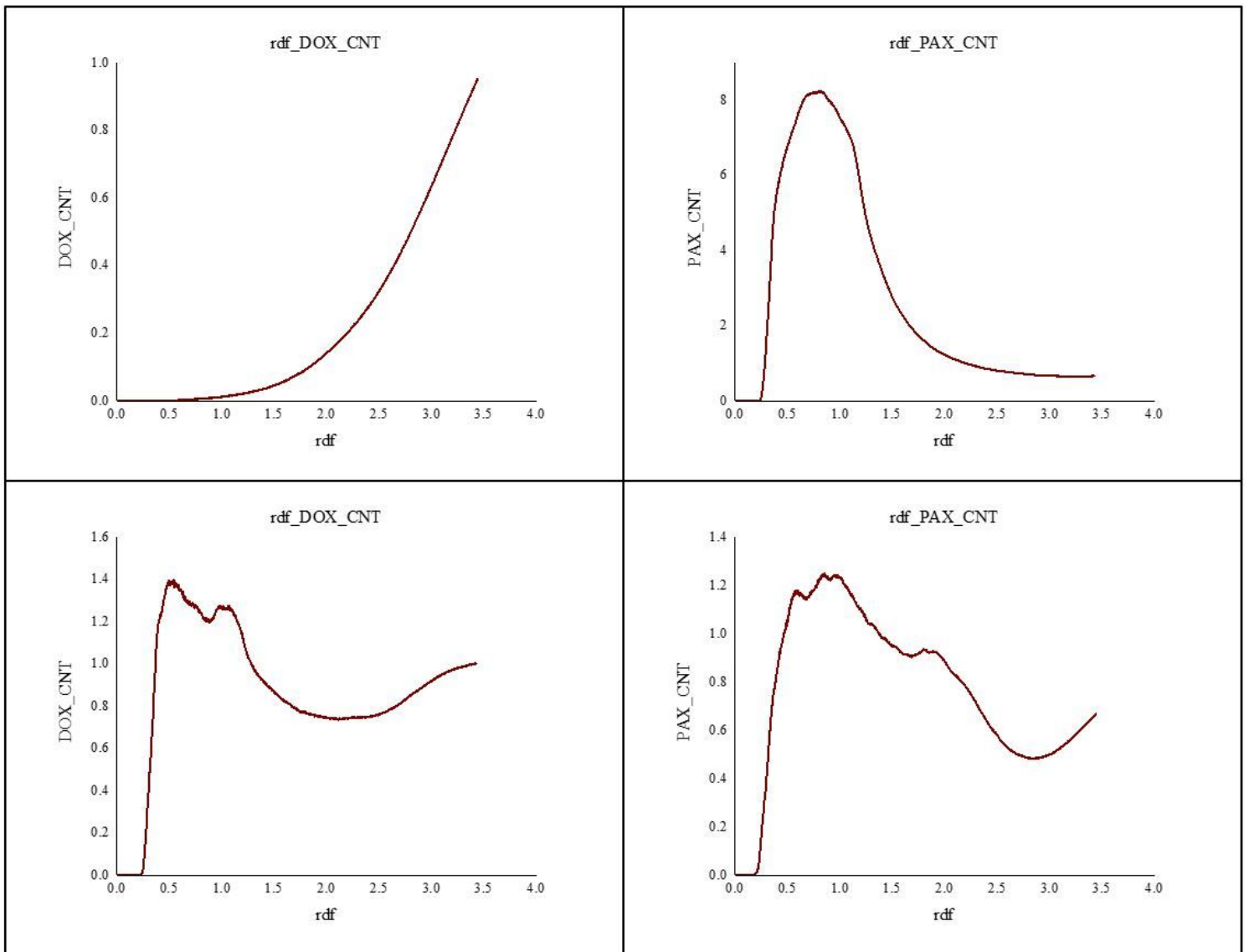


Figure 6

The RDF value of drugs and CNT a: DOX-CNT pH=7.4 b: PAX-CNT pH=7.4 c: DOX-PAX pH=5.5 d: PAX-CNT pH=5.5

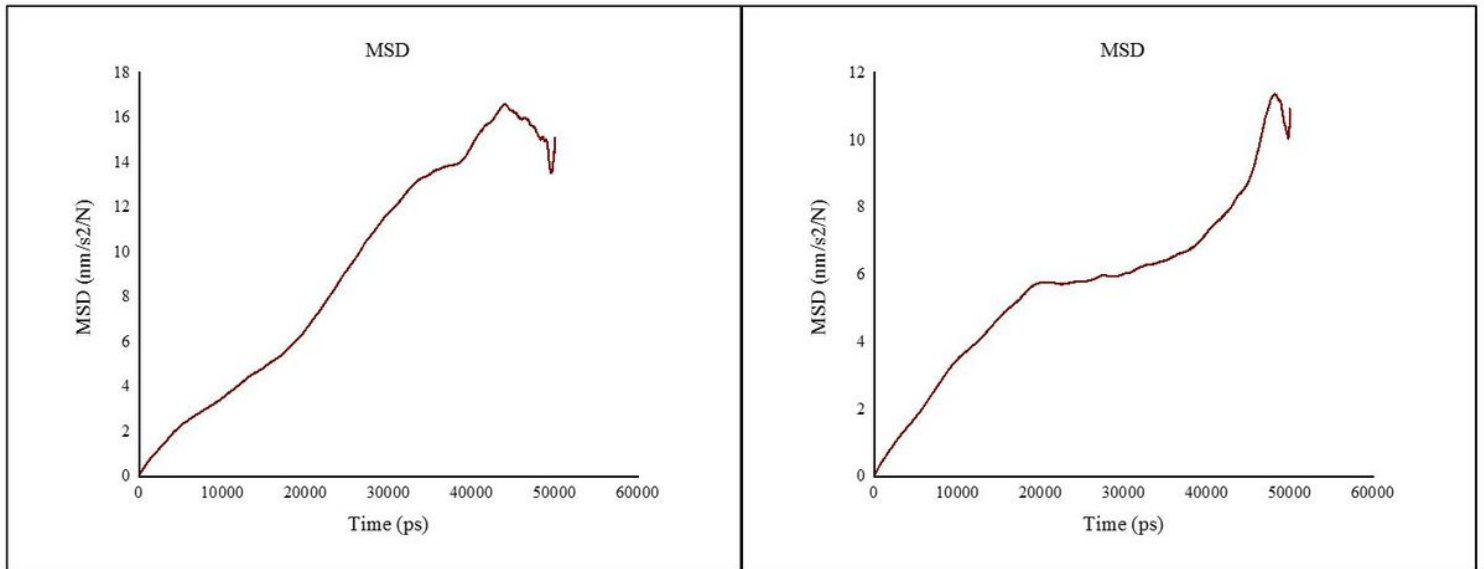


Figure 7

mean square displacement for DOX at a; pH=7.4 b:5.5

Supplementary Files

This is a list of supplementary files associated with this preprint. Click to download.

- [GraphicalAbstract.docx](#)